Journal of Molecular Structure 1080 (2015) 14–23

Contents lists available at ScienceDirect

Journal of Molecular Structure

journal homepage: www.elsevier.com/locate/molstruc

The role of Zundel-like ions in the supramolecular self-organization of porphyrin assemblies

Alexander V. Udal'tsov [a,*], Anastasia V. Bolshakova [b], Johannes G. Vos [c]

[a] Faculty of Biology, Lomonosov Moscow State University, Moscow 119899, Russia
[b] Chemistry of Polymers, Faculty of Chemistry, Lomonosov Moscow State University, Moscow 119899, Russia
[c] School of Chemical Sciences, Dublin City University, Dublin 9, Ireland

HIGHLIGHTS

- IR spectra indicate that $H_5O_2^+$ ions embedded in the cage between TPP units form stable clusters.
- A doublet at 2993, 3009 cm^{-1} confirms deuterium labeling of water clusters in the cage.
- IR studies of aggregates identify a doublet at 982, 1000 cm^{-1} with proton sharing in $H_5O_2^+$ ions.
- A mechanism for proton moving in water is suggested to explain a slanting cross with 55°.
- An estimate of proton hopping time of 6.4-7.9 ps supports this mechanism in the aggregates.

GRAPHICAL ABSTRACT

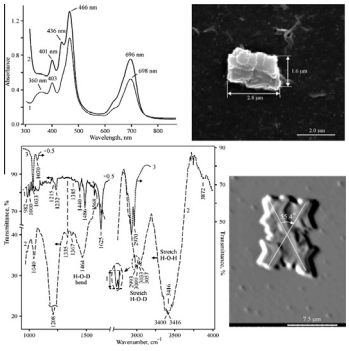

ARTICLE INFO

Article history:
Received 3 August 2014
Received in revised form 21 September 2014
Accepted 22 September 2014
Available online 28 September 2014

Keywords:
Protonated TPP dimers
Zundel-like ions
Self-organization
Confined water
Proton moving

ABSTRACT

Aggregates mainly consisting of mono-protonated *meso*-tetraphenylporphine (TPP) dimers and water self-assembled from the dimers in 0.4 N aqueous HCl with 0.86 mol L^{-1} tetrahydrofuran have been investigated by means of infrared spectroscopy (IR), electronic absorption spectroscopy, and scanning electron microscopy (SEM). IR studies using deuterium labeling of small-size protonated water clusters located in the cage between TPP in the dimers allow for the assignment of a doublet at 2993, 3009 cm^{-1} to stretching vibrations of H···O—DH and H···O^+—DH, respectively. In the absence of heavy water in the thin film a doublet at 982, 1000 cm^{-1} with the same energy gap of 16–18 cm^{-1} is identified with proton sharing in the O—H^+···O moiety of the cluster. The main features of the dimers, which provide their hydration, are the protonated —N= groups of pyrrole rings observed in the IR near 1486 cm^{-1} that are involved in the conjugated π-system of the porphyrin macrocycle. Stabilization of the electronic structure in the mono-protonated dimers occurs by $H_5O_2^+$ ions present in the cage between TPP units and charge delocalization through hydrogen bonding. It is proposed that together with the cooperative structure of the cluster the $H_5O_2^+$ ions are responsible for efficient self-assembling and self-organization of the highly ordered aggregates obtained. Based on surface studies a molecular mechanism for proton mobility is suggested to explain the origin of a slanting cross with the angle of 55° ± 3°, half the tetrahedral angle, on the surface of the aggregates in the solid state. Estimated proton hopping times of within 6.4–7.9 ps supports this molecular mechanism.

* Corresponding author at: Kominterna Str., 9-2-29, Moscow 129327, Russia.
Mobile: +7 8 926 685 1872.
E-mail address: avu151@yandex.ru (A.V. Udal'tsov).

http://dx.doi.org/10.1016/j.molstruc.2014.09.068
0022-2860/

Introduction

Water is a prerequisite for life and plays a central role in the determination of the structure and properties of living cells. As a result the vibrational characteristics of protonated water clusters have been investigated by many researchers to understand water's unique properties [1–5]. Small-size water clusters usually interact with a hydrogen ion to form species such as $H_5O_2^+$ or $H_9O_4^+$, the so-called Zundel and Eigen cations, respectively. The importance of these ions is their ability of proton sharing between water molecules in these small-size clusters [1–3]. In vibrational spectra of Zundel-like ions proton sharing is identified by a specific doublet near 1000 cm^{-1} that is connected with the proton-transfer mode [3–4]. Such a doublet was observed in resonance Raman and IR spectra of protonated TPP aggregates assembled from water–porphyrin dimeric complexes in solution and thin films [5]. These aggregates show an ordered surface structure including a slanting cross on the surface of the aggregates with an angle of 55° ± 3°, half the tetrahedral angle, but the origin of this structure was not well understood because of the absence of a molecular mechanism capable of explaining the angle of the slanting cross. In this paper we present further results revealing new features, which indicate that self-organization of water–porphyrin dimeric complexes into supramolecular structures can be explained by the specific properties of Zundel cations.

Previous results

In the dimeric complex [5] there are four —N= groups of pyrrole rings that can be protonated upon full protonation. However, in fact the full protonation does not take place because a squeeze of the network of the hydrogen bonds around TPP dimers and the hydrogen bonds connecting two TPP units restrict the full protonation. This hydrogen bonding defines only two configurations of the TPP dimers, with parallel and anti-parallel orientation of the dipole moments. So that the existence of two pairs of the positive charges in the cage between two hydrophobic TPP units upon full protonation is impossible simultaneously with the hydrogen bonding due to that the complex exists. Thus, in fact the features of the complexes formation restrict the full protonation of the dimers. That is why the dimers of this type were called as restrictively protonated species [6]. So-called restrictively protonated porphyrin dimers were initially found in solutions of *meso*-tetra(*p*-aminophenyl)porphine (TAPP) and TAPP covalently bound with a copolymer [7–8]. TAPP molecules in organic solvents usually form associated species because they contain amino-groups in *para*-position so that TAPP units are connected by hydrogen bonds via water molecules. For example, a monocation of the amino-porphyrin, which exists mainly in the dimeric state (λ_{max} = 430 nm for Soret band), has been found in aqueous dimethylformamide–ethanol solution by titration of a TAPP bound with a copolymer [7]. In this case two main absorption bands with λ_{max} = 462 and 757 nm were observed in the electronic spectra. The mono-cation radical of the TAPP dimer with λ_{max} = 463 and 735 nm was found when the porphyrin was oxidized with molecular bromine [8]. A di-protonated TPP dimer with λ_{max} = 437 nm for Soret band was observed in 50% (v/v) aqueous dioxane in a study of the dimerization of TPP resulting in the formation of $TPP_2H_2^{2+}$ [6], with a high dimerization constant of 1.9×10^9 mol^{-1} L. Mono-protonated TPP dimers with Soret bands at 403 and 465 nm related to parallel and anti-parallel configurations of their dipole moments, respectively, have been found at a higher water concentrations [6,9], when hydrophobic interaction between TPP molecules is considerably stronger. The pK_a for the protonation of —N= groups of pyrrole rings in a hydrophobic environment is considerable diminished, and a pK_a = 0.8 was found upon titration of TAPP bound to a hydrophobic/hydrophilic copolymer [10]. A doublet at 1000, 1025 cm^{-1} with the narrowed 1000 cm^{-1} component and a slightly higher intensity relative to the neighboring one was revealed in resonance Raman spectra of protonated TPP aggregates [11]. IR spectra of the aggregates in thin films usually demonstrate a doublet at 984, 1000 cm^{-1} [5]. The aggregates obtained were characterized using infrared and electronic spectroscopy and by scanning electron microscopy.

Materials and methods

All chemicals and organic solvents were of high-grade purity. Highly purified de-ionized water with a resistance of more than 18 MΩ was used for the producing of protonated TPP aggregates in aqueous 0.4 N HCl with a small concentration of tetrahydrofuran (THF). Thin films were obtained under evaporation of a solvent from the solution containing the aggregates with a warm stream of air to fix tracks of molecular motions on the surface. In this study our aim was to obtain aggregates with tracks on their surface that suggests a water–porphyrin matrix ordering. In these studies drying was needed to remove weakly bound water from the largely hydrated aggregates. However, complete drying of the layers creates aggregates that cannot be used for X-ray diffraction because they are possibly amorphous. A criterion of complete drying is a splitting of the bands of stretching and H—O—H bending vibrations of ordinary water as observed in IR spectra [9]. This requires an additional 2–3 min drying after water has disappeared from the surface. The splitting indicates that only water firmly bound in the aggregates is present. Typical approximately 1200 water molecules are found in the aqueous shell around each protonated TPP dimer in a completely dried thin film [9]. Weakly bound water in the films remains when the drying was stopped as soon as water has been disappeared from the surface of a film. Therefore, the water content in such not completely dried films is usually larger by 20% relative to that in a film obtained after complete drying of the sample [9]. IR spectra were recorded with a Specord M-80 spectrophotometer with an accuracy of 2–3 cm^{-1}. The complete drying method was also applied for thin films intended for SEM. Images of porphyrin aggregates were obtained with a Hitachi S-520 scanning electron microscope. The microphotographs were obtained with a side illumination for the images contrasting. All other experimental details have been reported before [5,9,12].

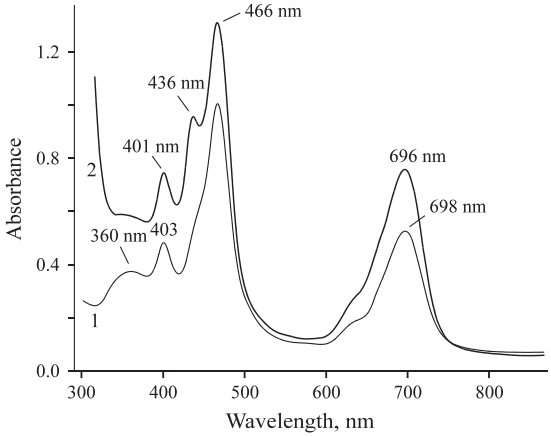

Fig. 1. Electronic absorption spectra of protonated TPP aggregates in (1) 0.4 N aqueous HCl with 0.86 mol L^{-1} THF; and in (2) D_2O containing 0.4 N HCl with 1.9 mol L^{-1} H_2O and 0.80 mol L^{-1} THF.

Results

Electronic absorption spectra shown in Fig. 1 demonstrate the usual characteristic features of protonated TPP aggregates in H_2O–THF and D_2O–THF solutions in the presence of 0.4 N HCl. The broad band with a λ_{max} = 360 nm that indicates the presence of the protonated state of TPP dimers (curve 1), is masked by the slope of the strong absorption of D_2O in curve 2. Two Soret bands with maxima at 403 nm and 465 nm (±1–2 nm) assigned to the mono-protonated TPP dimers with parallel and anti-parallel configurations of their dipole moments, respectively, are observed in both spectra. The third Soret band indicating the presence of di-protonated TPP dimer usually observed at λ_{max} = 437 nm and associated with an anti-parallel configuration of dipole moments is seen as a local maximum in curve 2. It should be noted that in the solutions the dimers are already assembled in the aggregates since they are formed immediately after the solution mixing. The concentration of the di-protonated TPP dimer is very low in H_2O–THF solution since only a very weak shoulder is noted in curve 1. In the red region of the spectra the bands of the protonated species are strongly overlapping producing one broad band with the maximum at 696 nm (±2 nm) and a shoulder around 630–635 nm.

Fig. 2 demonstrates that the protonated TPP aggregates can only be produced as a result of irreversible self-assembling of TPP dimers that are surrounded by an aqueous layer. The electronic spectrum of the di-protonated TPP dimer with the anti-parallel configuration in Fig. 2 (curve 1) exhibits two main bands with λ_{max} = 437 and 650 nm and no aggregates were observed in the solution. As expected hydrophobic interactions are not strong in a 50:50 water/dioxane solution as with a 67% water content as displayed in Fig. 2 (curve 2) or with 0.86 mol L^{-1} THF (7%, v/v) in Fig. 1 (curve 1). A higher concentration of 0.27 N HCl relative to 0.2 N HCl is not sufficient for protonation of TPP in the solution containing 33% dioxane as displayed in Fig. 2 (curve 2). Three bands of quasi-allowed electron transitions with maxima at ca. 528, 556, and 598 nm, which are red-shifted by 10–14 nm relative to those of $Q_y(0,1)$, $Q_y(0,0)$, and $Q_x(0,1)$ electron transitions of TPP, indicate the presence of neutral TPP molecules in the aggregates under these conditions. The maxima of these Q-bands of monomeric TPP in dioxane are observed at 514, 546, 588 nm, respectively as shown in curve 3. The fourth $Q_x(0,0)$ transition expected for neutral TPP at 647 nm in curve 3 overlaps with the band of the protonated TPP dimer with λ_{max} = 650 nm in curve 2. Importantly, in 0.27 N HCl the presence of neutral TPP units in the aggregates implies that their dimerization competes with the protonation of —N= groups of pyrrole rings during the self-assembling process. While formation of a hydration shell around the dimers prevents access of the excess of the ions in the solution to the pyrrole rings. Hence, the irreversible self-assembling of the dimers prevents reversible TPP ionization. Under these conditions a pK_a value is not defined. Furthermore, titration of a solution with the aggregates will lead to their decomposition and the precipitation of neutral TPP.

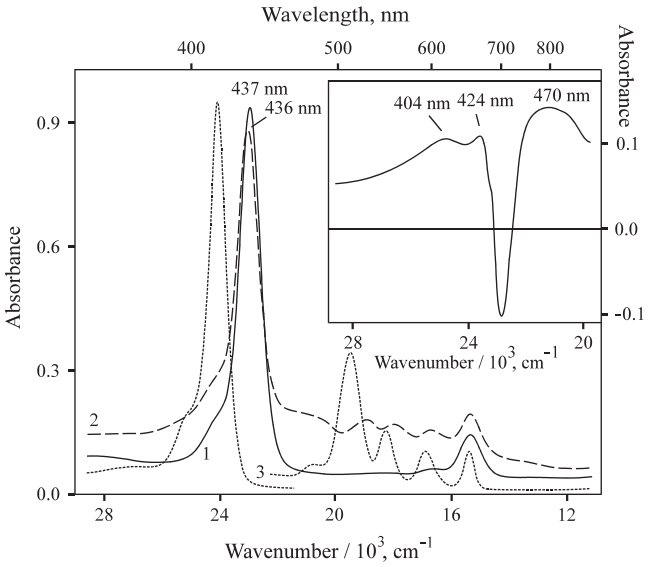

Fig. 2. Electronic absorption spectra of protonated TPP forms in (1) 0.2 N aqueous HCl with 50% (v/v) dioxane; and in (2) 0.27 N aqueous HCl with 33% (v/v) dioxane and (3) TPP in dioxane. Inset shows the difference spectra (curve 2 minus curve 1), optical pathlength was 0.1 cm.

The difference spectrum in Fig. 2 (inset) shows a red-shifted local maximum at 470 nm of mono-protonated TPP dimer and a maximum at 424 nm that is also red-shifted relative to λ_{max} = 417 - nm of Soret band of the neutral monomeric TPP. These features indicate that aggregates of neutral TPP with the protonated species are formed in the solution because of the spontaneous irreversible process. This also demonstrates that protons cannot penetrate through the hydration shell to pyrrole rings in the aggregates for the protonation of neutral TPP. It should be reminded that a proton is always hydrated in aqueous solutions. The effective ionic diameter of hydroxonium ion is 0.2 nm [13] but hydrophobic TPP molecules in a dimer surrounded by the aqueous shell with the tetrahedral network of hydrogen bonds are strongly compressed and this explains the restrictive character of TPP protonation [6]. On the other hand it has been established that $H_5O_2^+$ and $H_3O_2^-$ are the simplest ions in aqueous solutions of acids and bases [14] while in fact H_3O^+ and OH^- are absent. Therefore, the Zundel-type cation cannot penetrate to pyrrole rings for the protonation when the aggregates (Fig. 2, curve 2) have been formed in the result of the irreversible self-assembling.

IR spectra of protonated TPP aggregates in thin films displayed in Fig. 3 exhibit a splitting of H—O—H bending and stretching vibrations as shown in curve 1. The doublets at 1608, 1632 cm^{-1} and 3455, 3511 cm^{-1}, respectively, are observed but these stretching vibrations are not split when D_2O is used (curve 2). Under these conditions a broad band at 3416 cm^{-1} indicates that heavy water has been fully evaporated during the film preparation and only HDO remains in the ordinary water that is confined in the aggregates. This is confirmed by the ratios of the H_2O/HDO frequencies of combination vibrations indicated in Table 1. A blue shift of the 2256 cm^{-1} band in curve 3 relative to the 2152 cm^{-1} band in curve 1 is evidence of the weakening of hydrogen bonding in the solid thin film containing HDO. Because of this weakening of the interaction between water units the doublets observed in Fig. 3, curve 1 are not present in the presence of HDO as shown in curve 2. The vibration bands associated with the phenyl rings observed at 1568 and 1527 cm^{-1} in Fig. 3 (curve 1) are red shifted by 24–25 cm^{-1} relative to those at 1592 and 1552 cm^{-1} in the IR spectra of TPP in KBr [15] indicating hydration of the phenyl rings in the film. In contrast, four small bands at 1568, 1552, 1537, 1512 cm^{-1} in Fig 3 (curve 3) point to the hydration of phenyl rings involving HDO. A very small peak at 1415 cm^{-1} corresponds to the most intense band at 1568 cm^{-1} (see the Table 1), 1568/1415 = 1.108 or 1592/1415 = 1.125 proving HDO labeling. So, H_2O and HDO species present close to the phenyl rings are mainly grouped in clusters of a mixed composition since two additional somewhat shifted bands are noted. The $N_tH^+\cdots OH_2$ bond No 1 in Table 1 (or $N_t^+H\cdots OH_2$ if to be more exact), in which the tertiary nitrogen atom (N_t) is interacting with the conjugated 18-electron π-system of TPP macrocycle, is shown to be insensitive to deuterium labeling (Ratio = 1.007). The bands at 1479 and 1433 cm^{-1}

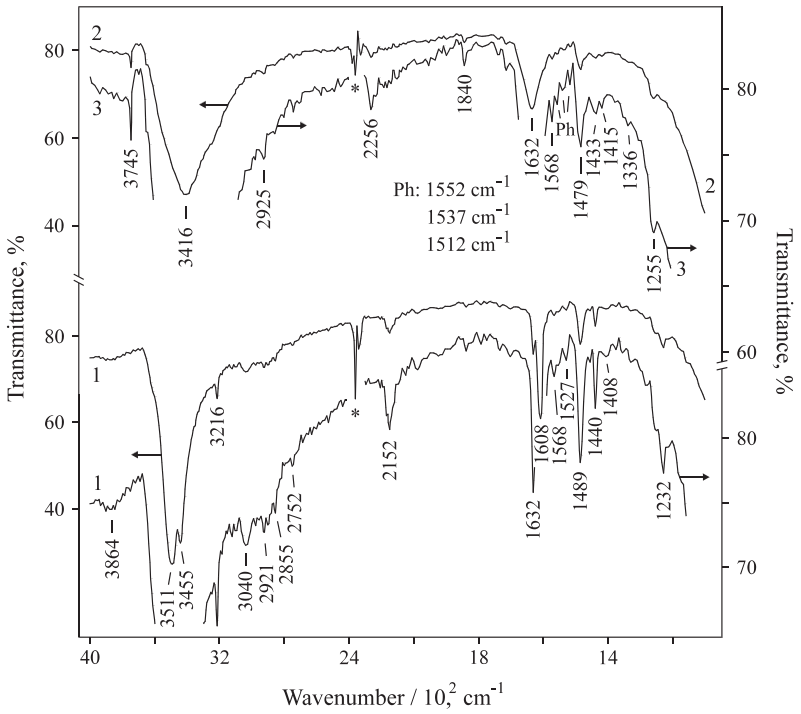

Fig. 3. IR spectra of protonated TPP aggregates in thin films prepared on CaF_2 by evaporation of (1) 0.4 N aqueous HCl with 0.86 mol L^{-1} THF; and (2, 3) D_2O containing 0.4 N HCl with 1.9 mol L^{-1} H_2O and 0.80 mol L^{-1} THF; both films were completely dried. Arrows mark the corresponding left and right transmittance scales; Ph is the solvated phenyl rings. An asterisk marks atmospheric CO_2.

Table 1
Ratios of the frequencies of H_2O and HDO involved in the different bonds; the frequencies are taken from Figs. 3 and 4. Tertiary and secondary nitrogen atoms are abbreviated as N_t and N_s, respectively.

No	Bond vibrations	Frequencies, ν_{H-O-H}/ν_{H-O-D}	Ratio, ν_{H-O-H}/ν_{H-O-D}
1	$N_t^+H\cdots OH_2/N_t^+H\cdots ODH$	1489/1479	1.007
1	Stretch $N_t^+H\cdots OH_2/N_t^+H\cdots ODH$	3057/3033	1.008
2	$N_t\cdots H_3O^+/N_t\cdots H_2DO^+$	1489/1336	1.115
2	$N_t\cdots H_3O^+/N_t\cdots H_2DO^+$	1486/1335	1.113
3	Solvated C_6H_5 ring	1568/1415	1.108
4	Combinations, L + bend[a]	2152/1840	1.170
4	Combinations, L + bend[a]	2256[b]/1840	1.226
5	Stretch H—O—H/H—O—D	3416/3022[c]	1.130
6	Bend H—O—H/H—O—D	1644/1464	1.123
7	Stretch $H\cdots O—H_2/H\cdots O—DH$	3400/2993	1.136
8	Stretch $H\cdots O^+—H_3/H\cdots O^+—DH_2$	3416/3009	1.135
9	Stretch $N_s—H\cdots OH_2/N_s—H\cdots O—DH$	1232[d]/1040	1.185
10	Stretch $N_t\cdots H—OH/N_t\cdots H—OD$	1215[d]/1040	1.168

[a] The combination of librations and H—O—H/H—O—D bending vibrations.
[b] The blue shifted band from Fig. 3 (curve 3).
[c] The centered frequency of the HDO band.
[d] Tentative assignment since it is impossible to identify this frequency with $N_s—H\cdots OH_2$ or $N_t\cdots H—OH$ exactly.

in curve 3 are only red shifted by 7–10 cm^{-1} relatively the corresponding bands in curve 1. In contrast, the $N_t\cdots H_3O^+$ bond (No 2 in the Table 1) is sensitive to the labeling, with a Ratio = 1.115. These two bonds are the extreme structures for proton sharing in the $N_t\cdots H^+\cdots O$ moiety, see Scheme 1 (I) and the frequency of the former is defined by the properties of protonated state of the tertiary nitrogen atom. Hence, when the proton is delocalized within the 18-electron π-system its frequency is independent from deuterium labeling.

The IR spectrum of the aggregates with not completely dried thin films (Fig. 4, curve 1) shows the doublet at 982, 1000 cm^{-1}, which as suggested in [5] arises from $H_5O_2^+$ incorporated in the cage of protonated TPP dimers and prevents the hydrophobic TPP molecules from the precipitation in the aqueous solution. Importantly a water coating around each dimer consisting of ca. 1200 H_2O [9] is a prerequisite for quick self-assembling of the protonated dimers into the aggregates. The vibrational behavior of the water in water–porphyrin dimeric species formed upon $H_5O_2^+$ incorporation is much more complex than that of freely moving Zundel cations since its main state is defined by the properties of the protonated tertiary (N_t) nitrogen groups. In contrast with what is observed for the bare Zundel cation, in these porphyrin based assemblies equal proton sharing is impossible since there is always a porphyrin based proton-accepting group (—N= or OH_2) competing for a proton.

The IR spectrum of the aggregates prepared with D_2O in solution (Fig. 4, curve 2) exhibits a red-shifted 1335 cm^{-1} band assigned to the $N_t\cdots H_2DO^+$ bond (No 2 in the Table 1). The neighboring 1367 cm^{-1} band suggests the presence of HDO-solvated phenyl rings (1568/1367 = 1.147) because the 1364 cm^{-1} band in

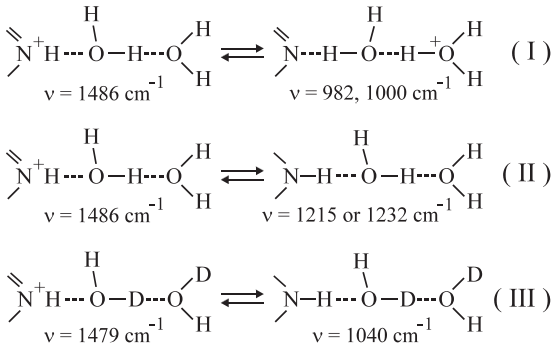

Scheme 1. The extreme structures of protonated nitrogen atom (I) interacting with water dimer in the cage between TPP units and (II), (III) under NH-tautomeric transitions, and under deuterium labeling (III). Hydrogen bonds are depicted by dotted lines.

IR spectrum of THF has very weak intensity and cannot be seen at a small concentration as 0.80 mol L^{-1} THF. The doublet at 1440, 1486 cm^{-1} observed in curve 1 is masked in curve 2 by the 1464 cm^{-1} band, so only weak shoulders are noted.

A doublet at 2993, 3009 cm^{-1} with an energy gap of about 16 cm^{-1} between the components as observed for the doublet near 1000 cm^{-1} is found in the region of H—O—D stretching vibrations in Fig. 4 (curve 2). This doublet has the same narrowed high-frequency component (3009 cm^{-1}) similar as that observed for the band at 1000 cm^{-1} in curve 1 and has a similar shape. The 2993, 3009 cm^{-1} doublet is assigned to the stretching vibrations of H···O—DH and H···O^+—DH_2 bonds, see the Table 1, No 7 and 8, respectively. In solution there are no fixed structures for small-size water clusters such as those found in the cage between TPP units of the dimers because in solution the proton is usually delocalized. So in solution only the small-size clusters embedded in the cage are observed in the IR spectrum. Interpretation of this small doublet in terms of the positive Fermi resonance suggests that hydrogen bonding in HDO···H—O^+DH units embedded in the cage between TPP units is also stronger since clusters are formed. The relative intensity for the components in the different doublets is equal, $I^{982}/I^{1000} = 0.91$ and $I^{2993}/I^{3009} = 0.91$ taking into account the inclined baseline in the former. In resonance Raman spectra [11] for the doublet near 1000 cm^{-1} the ratio of I^{1025}/I^{1000} was found to be the same ($I^{1025}/I^{1000} = 0.91$), values are averaged for aggregates in different solvents. This behavior is in an agreement with the fact that in Raman spectroscopy the intensity of a band is proportional to polarizability of a molecule while in IR spectra it is proportional to the dipole moment. These and above results allow identifying the doublet near 1000 cm^{-1} with the proton sharing in the O···H^+···O moiety of a Zundel cation that is located in the cage between TPP units, see Scheme 1(I). The assignment of the narrowed component to an extreme structure as a O···H—O^+H_2 moiety is supported by the following observations. The appearance of a band at 1033 cm^{-1} in the IR spectrum of fully dried triethylammonium chloride shown in Fig. 4 (curve 3) indicates the presence of H_3O^+ only because the proton is usually hydrated. But a second H_2O in $Et_3NH_3O^+Cl^-$ is absent and the low-frequency component in the vicinity in the IR spectrum is absent too. Importantly the absence of the second H_2O prevents Zundel cation formation. The hydroxonium ions and Zundel cations have been often found in crystals [16], for instance, in crystals of perchlorates the 1020 cm^{-1} band of H_3O^+ was shifted to 945 cm^{-1} in H_2DO^+.

The 3040 cm^{-1} band observed for the TPP aggregates shown in Fig. 3 (curve 1) is assigned to vibrations of the protonated tertiary nitrogen atom [17] that is usually present in IR spectra of aliphatic amines, $alkyl_3NH^+$. But the IR spectrum of fully dried $Et_3NH_3O^+Cl^-$ in Fig. 4 (curve 3) does not show such a band, the presence of which requires the presence of a second H_2O or HDO molecule. Instead, two small bands at 3033 and 3057 cm^{-1} are observed in

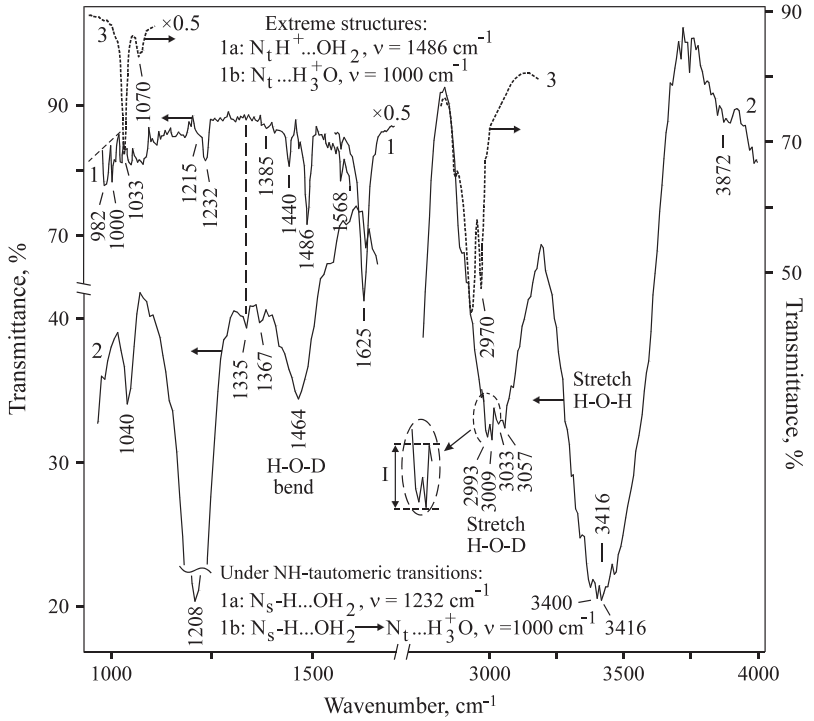

Fig. 4. IR spectra of protonated TPP aggregates in (1) not completely dried thin film prepared on CaF_2 by evaporation of 0.4 N aqueous HCl with 0.86 mol L^{-1} THF, (1) is the difference spectrum of the film on CaF_2 minus that of CaF_2 recorded as a background; and in (2) D_2O containing 0.4 N HCl with 1.9 mol L^{-1} H_2O and 0.80 mol L^{-1} THF; and (3) fully dried triethylammonium chloride in KBr. The IR spectrum of THF showed intense C—H stretching vibrations peaked at 2962 and 2853 cm^{-1} and a weak and very weak bending ones at 1460 and 1364 cm^{-1}, respectively.

Fig. 4, curve 2. As mentioned above the $N_t^+H\cdots OH_2$ bond is insensitive to the deuterium labeling (see the Table 1, No 1). The deuterium labeling effect can be seen in IR spectra when hydrogen bonding with a second H_2O or HDO takes place. Therefore, the presence of structures such as $N_t\cdots H_3O^+$ or $N_t\cdots H_2DO^+$ (No 2) imply proton sharing in $H_2O{-}H^+\cdots OH_2$ or $HDO{-}H^+\cdots OH_2$ bonds interacting with N_t. The relation between intensities of the bands at 1479 and 1336 cm^{-1} in Fig. 3 (curve 3) indicates that the main state is that when proton is bound to the tertiary nitrogen atom. It should be noted that in the water–porphyrin dimeric complex the $H_2O{-}H^+\cdots OH_2$ bond is an intermediate state, which emerges under proton transfer to the neighboring TPP in the dimer.

Vibrations of the N—H groups of pyrrole rings in TPP at 3216 cm^{-1} observed in Fig. 3, curve 1 are not seen in curves 2 and 3 although there are four such groups in mono-protonated TPP dimer. As suggested earlier [5] stabilization of the electronic structure of mono-protonated TPP in the dimer can occur due to the polarization of the H_2O molecule bound in the complex that causes the appearance of the 1232 cm^{-1} band and favors NH-tautomeric transitions, Scheme 1 (II). The neighboring shoulder at 1215 cm^{-1} observed in Fig. 4, curve 1 can be assigned to vibrations of the $N_t\cdots H{-}OH$ bond, see Table 1, No 10. The IR spectrum in Fig. 4 (curve 2) shows the 1040 cm^{-1} band associated to such labeled bonds, see the Table 1, No 9 and 10, and the Scheme 1 (III). The 1040 cm^{-1} band is more intense relatively to the 1335 cm^{-1} peak because there are four N—H and again three —N= groups coordinated with H_2O, see Scheme 2. So, the observed intensities are in an agreement with this when taking into account the 7-fold larger content of $N_s{-}H\cdots O{-}DH$ and $N_t\cdots H{-}O{-}D$ bonds in the dimer relative to that of $N_t\cdots H_2DO^+$ one. The latter is shown in the Table 1 and in the Scheme 2. Note that there is no appreciable signal around the 1335 cm^{-1} area in the IR spectrum of the thin film without labeling in Fig. 4 (curve 1). Hence, hydrogen bonded water molecules in the cage between TPP in the dimers are mainly involved in the stretching vibrations because they hold the neighboring TPP units in the dimeric state and at the same time prevent TPP from the precipitation. The above features can be summarized in the following Scheme 2.

Water molecules of the coating around the dimer form a network of hydrogen bonds created by donor–acceptor interactions between water molecules confined in the aggregates are enhanced under the complete drying. This leads to the splitting of the water's vibration bands as shown in Fig. 3 (curve 1). Note that as a result of deuterium labeling the narrowed 3745 cm^{-1} band in curves 2 and 3 indicates dangling O—H groups [18] that implies some distortion in the network of clusters involving HDO. It should be noted that the state of water confined in the aggregates is connected with the protons ability to move in the water coating surrounding the porphyrin dimers. The fact is that the protons are not restricted in their movement as long as the solvent is not completely evaporated so the traces of molecular motions are mirrored in the solid state of thin film [5]. The presence of proton sharing in Zundel-like ions is a prerequisite for the proton moving through the water coating of the dimers a process that depends on the water content in the thin film.

Let us consider features of proton delocalization in details. In the 18-electron π-system of the conjugated bonds electrons are delocalized over the porphyrin macrocycle. There are only two possibilities for proton interactions when a tertiary nitrogen atom in the dimer has been protonated. The first is that when proton interacts with a water molecule of the cluster in the cage. In this case vibrations of the $N_t\cdots H_3O^+$ bond are sensitive to deuterium labeling as found above. And the second is that when proton interacts with an electron delocalized over the π-system since both N_t

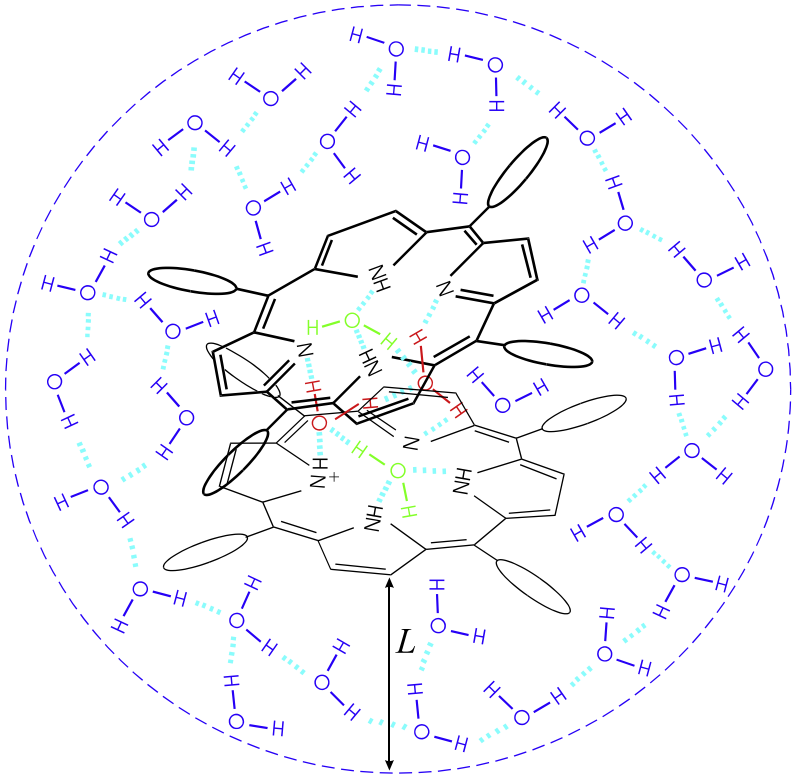

Scheme 2. Structure of water–porphyrin dimeric complex surrounded by the water coating proposed for a mono-protonated TPP dimer containing a *cis*-NH-tautomer [5]. The thickness (L) of the water layer around the dimer was estimated using water density of 0.0333 $Å^{-3}$ and number of H_2O in the layer equaled 1260 [9], L = 2.0 nm. Two water molecules bound with H^+ and tertiary nitrogen atoms and other two H_2O in the cage are shown by red and green, respectively. Hydrogen bonds are depicted by dotted lines. (For interpretation of the references to color in this figure legend, the reader is referred to the web version of this article.)

in TPP molecule are included in the conjugated π-system. In this case the proton has to be in the coupled state with an electron of the π-system due to the interaction between positive and negative charges. Therefore, this proton is delocalized over the conjugated π-system in the coupled state with a π-electron that implies actual its movement along the conjugated bonds of the closed tetrapyrrole ring. This suggestion follows from the finding that the vibrations of the $N_t^+H\cdots OH_2$ bond are independent from deuterium labeling.

Hence, the results of IR spectroscopy show that vibrational properties of the TPP dimers are defined by the protonated state of tertiary nitrogen atom of a pyrrole ring. When proton leaves the conjugated π-system, the charged state of the dimer is distributed over the complex via hydrogen bonding with the small-size water cluster bound in the cage between TPP units. Therefore, stabilization of the electronic structure in the mono-protonated dimers occurs due to the charge delocalization in the porphyrin macrocycle and through the hydrogen bonding in the cage of the complex. These features of proton movement in the complex create favorable conditions for its movement through the water–porphyrin matrix, since protons have an opportunity to renew their energy for the moving along hydrogen bonds in the network, when the dimer absorbs a quantum of the light. Note, that the dimers are formed in the dark too, but the light is apparently needed for the effective self-organization of the structure. These features constitute a background of cooperative interactions and molecular motions under self-organization processes in solution.

It is important to note that in the present set of measurements the purity of the distilled water used was significantly better than observed in our earlier studies [9,12]. The present results were obtained in wintertime when iron water pipes underground are cooled by the frost. In this case the purity of distilled water proved to be substantially better than the twice-distilled water obtained during late spring–summer [12] or autumn time [9]. Fig. 5 shows structural features on the surface of protonated TPP aggregates, which are usually observed by SEM when aqueous THF is used as a solvent to generate them. The size of these aggregates is between 8 and 10–11 μm in the length while the size of the aggregates obtained in less pure distilled water was about 2–3 μm and but not exceeded 5–6 μm in the length [12]. An important feature in Fig. 5 is the presence of structural organization as manifested by a series of linear features on the surface of the aggregates. Other peculiar of the structural organization is a "swallow" tail of the smaller edge of the aggregate (on the left hand) that suggests a definite way of the matrix ordering.

When D_2O/H_2O mixtures with the molar ratio of 26/1 and with 0.8 mol L^{-1} THF are used as a solvent the size of protonated TPP aggregates is smaller and do usually not exceeded 3 μm in the length (Fig. 6). This feature is explained by donor–acceptor interactions with hydrogen bonding in the cage of TPP dimers surrounded by an ordinary water shell that is responsible for strengthening of the hydrogen bonding resulting in larger clusters. But in the case of heavy water weakening of hydrogen bonding takes place as evidenced by the 104 cm^{-1} blue shift of the 2256 cm^{-1} band in Fig. 3 (curve 3) relatively the 2152 cm^{-1} one in curve 1. This weakening of the hydrogen bond capacity results in a reduction of the size of water clusters. The HDO moieties are preferably involving in $N_sH\cdots O—DH$ and $N_t\cdots H—O—D$ bonds in the cage, as displayed by the 1040 cm^{-1} band in Fig. 4 (curve 2), and this weakens the structure of the dimeric complex. The 23 cm^{-1} blue shift of the 1255 cm^{-1} band in Fig. 3 (curve 3) relative to the 1232 cm^{-1} one in curve 1 just indicates such a weakening of the hydrogen bonding in the complex.

Layer organization in the aggregate shown in Fig. 6 formed in the presence of D_2O suggests that in this case protonated TPP dimers self-assemble preferably by stacking of the dimers due to hydrophobic interactions between the phenyl rings, because there are no linear structural features on the surface as observed in Fig. 5. The size of the layers in the aggregate varies between 500 and 1400 nm that indicates weak non-specific self-assembling properties. This implies that protons in the aqueous coat around the complex containing HDO moieties have limited mobility within the cluster possibly because of defects of hydrogen bonds network. As discussed above the presence of the 3745 cm^{-1} band representing dangling O—H groups in Fig. 3 (curve 3) is in agreement with this suggestion. In addition as a result of interaction between phenyl rings of the protonated TPP dimers formation of a larger number of shorter assemblies takes place. This creates an unordered water–porphyrin matrix because layers are separated from each other as seen in Fig. 6. Hence, in the presence of a great deal of heavy water the protons can only move within shorter distances

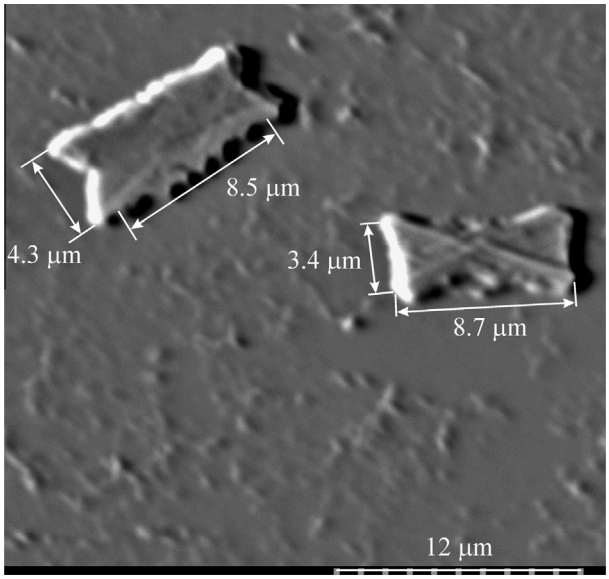

Fig. 5. SEM image of protonated TPP aggregates in thin film prepared by evaporation of 0.4 N aqueous HCl with 0.86 mol L^{-1} THF with the usage of fresh distilled water.

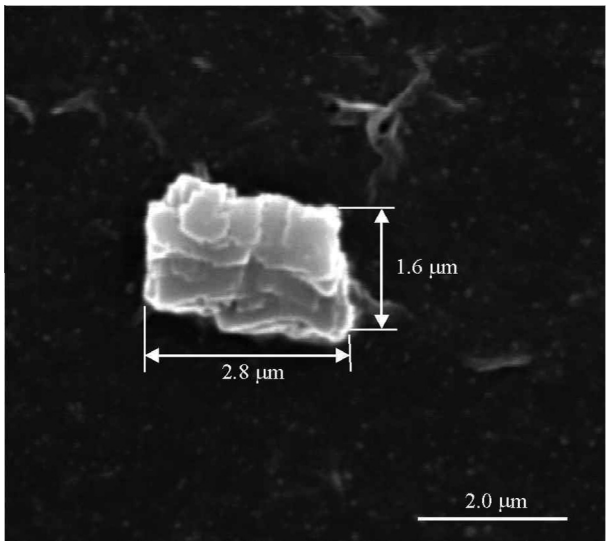

Fig. 6. SEM image of a single protonated TPP aggregate in thin film prepared by evaporation of D_2O containing 0.4 N HCl with 1.9 mol L^{-1} H_2O and 0.80 mol L^{-1} THF.

relative to those in the case of pure water composes the aqueous phase inside the coat around the water–porphyrin complex. The light illuminating the aggregates did not fall on the plate surface because of an appreciable thickness of the aggregates formed, so that the background in this image is black.

The structural organization of protonated TPP aggregate is dramatically changed when very pure water is used for producing the aggregates as outlined above. Under these conditions highly ordered surface structures with a slanting cross on the surface of aggregates are observed as in Fig. 7. The sharp angle of the slanting cross is 55° ± 3° on average [5]. This value is close to half of the tetrahedral angle of 109.5°, which defines the coordination of neighboring water molecules in a network of hydrogen bonds in ice and in the nearest order, i.e. first coordinating shell in the structure of liquid water [19]. The length of the aggregates is 10–12 μm and these values considerably exceed those in aggregates obtained in the presence of heavy water (Fig. 6). The ordered structure of the aggregates in Fig. 8 (on the right hand) and the slanting cross relate to the presence of water confined in the aggregates. The observed regular or irregular surface features reflect different speeds of the matrix ordering. This picture is typical for highly ordered water–porphyrin matrixes [5]. The width of the crossing lines of this aggregate (Fig. 8) is 360 nm on average.

The crossing lines observed in Fig. 8 and an ordered structure of the aggregate in Fig. 7 can be related to tracks of molecular motions that are fixed after solvent evaporation. They are most likely connected with protons moving through the water matrix presented around the dimers via a proton sharing mechanism involving the Zundel-like ions. This process can be accompanied by transitions between different NH-tautomeric forms. None of the different types of Grotthuss mechanisms for proton movement in liquid water [20] can explain the observed 55° angle.

In liquid water the tetrahedral coordination of water molecules is only maintained in the first coordination shell [19]. A tetrahedral coordination with a weak hydrogen bond bending (Θ angle = 101.5°, see Scheme 3), where Θ is the angle formed by lines connecting three neighboring oxygen atoms) was also assumed. Using a 2.98 Å oxygen–oxygen distance in liquid water structure [21] and a 2.36 Å oxygen–oxygen distance in Zundel cation [13], an estimate of the angle (alpha/2, in the Scheme 3) between direction of proton moving and a proton hopping step from one Zundel ion to its next position yields a value, which is in a good agreement with that observed in the images in Fig. 7 as shown below.

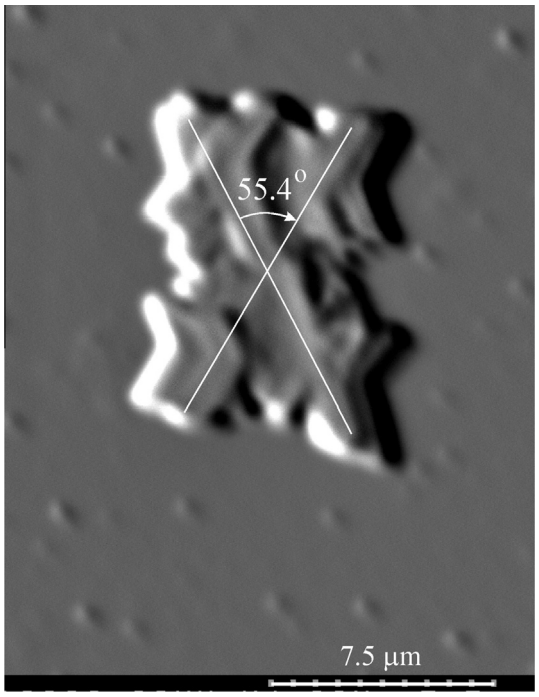

Fig. 7. SEM image of a single protonated TPP aggregate in thin film prepared by evaporation of 0.4 N aqueous HCl with 0.86 mol L^{-1} THF with the usage of highly purified water (distilled water was de-ionized after that its resistance was more than 18 MΩ.).

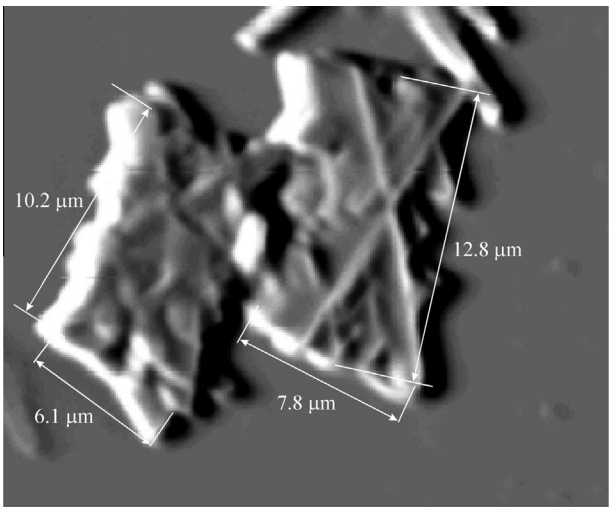

Fig. 8. SEM image of protonated TPP aggregates in thin film prepared by the same way as displayed in the caption of Fig. 7.

The proton moving direction in Scheme 3 is defined by the direction of vibrational motions in the original Zundel ion, i.e. by the line connecting its two oxygen atoms. If a proton hopping step occurs to the neighboring water molecule as in Scheme 3 left, then according to this scheme the calculation of the alpha angle yields a value of 89.4° that is too much of an angle for the H—O—H bending needed to allow hydrogen bonding with the neighboring oxygen atom. In this case a deviation for calculated alpha angle with the value observed is higher than 60%, (89.4° − 55°)/55° = 0.625. Therefore, the neighboring water molecule cannot be a proton-capturing species. Hence, proton moving via Zundel cation states along hydrogen bonds by Grotthuss mechanism [20] seems to be implausible because there is a restriction for the H—O—H angle bending under the hydrogen bonding regime. It should be noted that in fact Grotthuss mechanism is a relay-race type one [14,22] and this mechanism can be only applied to H_3O^+ for the explanation of proton anomalous mobility [23] or to $H_3O_2^-$ ion moving. Besides that the Grotthuss mechanism cannot be applied to an aqueous solution containing $H_5O_2^+$ [14] because in this case the synchronic transfer of two protons is required. Only in that case there will be no changes in the solution structure; a mechanism of the synchronic transfer of two protons has been considered [24]. In the case of proton tunneling the hydrogen bonding regime does not allow to apply the Grotthuss mechanism as argued above. Furthermore, the Grotthuss mechanism does not explain why the proton moves forward and cannot move in the backward direction after a hopping step in the absence of an electric field. Finally, proton transport involving Zundel ion and $H_3O_2^-$ ion moving by the same way along hydrogen bonds contradict the existence of aqueous ammonium hydroxide or aliphatic amines solutions with a high pH because the positive and negative charges will be recombined. An alternative pathway for proton movement is shown in the Scheme 3 at the right, where the proton bypasses the neighboring water molecule. For that process an alpha value of 52.4° is estimated which is within of the measurement error of the value of 55° observed in Fig. 7. The structure of each Zundel ion will have

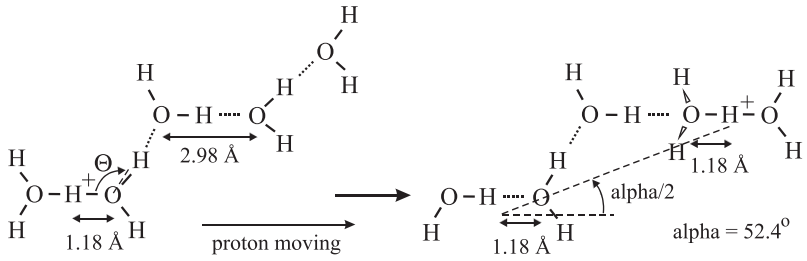

Scheme 3. Molecular mechanism proposed for proton mobility by a hopping step bypassing the neighboring water molecule that is in agreement with the experimental results.

to be oriented along the proton moving direction for this process to be effective. This implies a vibrational relaxation of each water molecule immediately after a proton accepting to form the Zundel ion structure after the proton-hopping step. The length/width ratio for all aggregates in the present work and in the previous one [5] except for those obtained in the presence of heavy water is found to be 1.91 ± 0.26 without taking into account the "swallow" tails contribution (see Fig. 5). This ratio is estimated to be 1.86 for Zundel cation and for the water dimer oriented in the direction in which the proton is moving (on the right side of the Scheme 3) a values of 2.08 is obtained, so an average value of 1.97 is in good agreement with the ratio measured for the aggregates. This suggests that the proton transfer direction coincides with the line of an aggregate length even the structural features are not observed on the surface. It should be noted that vibrational energy needed for such proton hopping steps could be accumulated from excited states of mono-protonated TPP dimers with different configuration, the exciton interaction energy of which is 1650 cm^{-1} [5]. Hence, proton movement proceeds along a chain of water molecules in the same direction as in the initial Zundel cation and is periodically accompanied by hydrogen bonding. This way of proton movement covers the distance of the whole aggregate as we can see from Figs. 5, 7 and 8. Thus, self-organization processes defining highly ordered molecular structure in the aggregates have a direct relationship with the unique liquid water structure which allows for efficient proton movement in the surrounding aqueous coatings. Tracks of these molecular motions are observed after solvent evaporation in the fixed solid state.

Scheme 3 allows an estimate of the mean time (τ_{ph}) between successive proton hopping steps using the Einstein–Smoluchowski equation (1) for a three-dimensional walk:

$$D_{H+} = l^2/6\ \tau_{ph} \quad (1)$$

where l is the mean step distance and D_{H+} is the proton diffusion coefficient. The latter can be calculated using the Stokes–Einstein equation (2):

$$D_{H+} = k_B T/(6\ \pi\eta R_p) \quad (2)$$

where k_B is Boltzmann constant, η is the dynamic viscosity of water (η = 0.894 cP [25] at 298 °K), R_p is the radius of the diffusing particle, the proton radius can be evaluated as follows. Fig. 9 shows a plot of oxygen–oxygen distance in Zundel cation versus effective reverse proton radius under diffusion. R_p was calculated as follows: $1/R_p = ((R^+_{(O-H-O)}/2) - 0.96\ Å)^{-1}$; where $R^+_{(O-H-O)}$ is the oxygen–oxygen distance in Zundel cation; 0.96 Å is the length of O—H bond; the $R^+_{(O-H-O)}$ values were taken from [4,13,26,27].

Dots, which are obeying the linear correlation (line 1) between the oxygen–oxygen distances within Zundel cations, correspond to proton sharing within the cations. As suggested the linear correlation (line 2) between the distances in small-size protonated water clusters corresponds not only to proton sharing between two water molecules but also the proton delocalization over the water clusters.

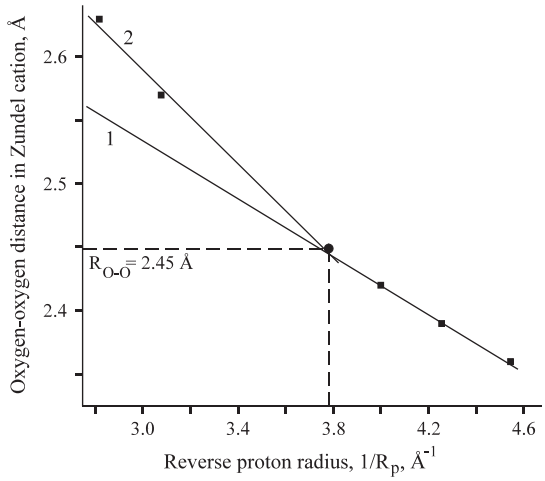

Fig. 9. Plot of oxygen–oxygen distance in Zundel cation versus the reverse proton radius ($1/R_p$). The latter was calculated as follows: $1/R_p = ((R^+_{(O-H-O)}/2) - 0.96\ Å)^{-1}$; where $R^+_{(O-H-O)}$ is the oxygen–oxygen distance in Zundel cation; 0.96 Å is the length of O—H bond.

The proton size of $2R_p$ = 0.529 Å is an effective diffusional one because the oxygen–oxygen distance in Zundel cation of 2.45 Å (0.529 Å + 2 × 0.96 Å = 2.449 Å) really means that the proton has an equal probability for sharing in the Zundel cation as for delocalization in liquid water structure since the oxygen–oxygen distance of 2.45 Å plus 0.53 Å gives the oxygen–oxygen distance of 2.98 Å in water. The positive charge delocalization over a water cluster has been found for $H(H_2O)^+_6$ ion with a high oxygen–oxygen distance of 2.57 Å in $(O—H—O)^+$ [26] that obeys line 2. The dot with half of Bohr radius (R_p = 0.529 Å/2) marked by circle in Fig. 9, corresponds to the value of $1/R_p$ = 3.78 $Å^{-1}$ and obeys both of these correlations. Hence the effective proton radius, R^{ef}_p = 0.529 Å/2 is an optimal value for the proton moving in water without structural restrictions. Substituting the values in the Eq. (2) we obtain $D_{H+} = 9.23 \times 10^{-5}$ $cm^2\ s^{-1}$ (or D_{H+} = 0.923 $Å^2$/ps). An experimental value of the proton diffusion coefficient of 0.94 ± 0.01 $Å^2$/ps has been reported in the literature [28]. The 4.3-fold higher value of the diffusion coefficient relative to the coefficient of water self-diffusion ($D_{water} = 2.13 \times 10^{-5}$ $cm^2\ s^{-1}$ at the same temperature [29]) suggests proton movement through water, especially if proton is really moving as a wave as implied in Scheme 3.

With regard to proton hopping steps, two different possibilities can occur, firstly when a water molecule captures a proton moving along the hypotenuse (l_h), or secondly along the line connecting two oxygens in the origin Zundel cation that defines the proton moving direction (l_{pmd}). A direction between l_h and l_{pmd} lines is most probable for the proton hopping step because otherwise agreement with the experimental results will be not obtained. Substituting the diffusion coefficient and the corresponding mean distance in Eq. (1) we have τ_{ph} = 7.90 ps in the former case and

τ_{ph} = 6.36 ps in the latter or τ_{ph} = 7.1 ps in average. The proton hopping rate defined as $k_{ph} = 1/\tau_{ph}$ is to be 1.4×10^{11} s^{-1} on average. In the both cases these proton hopping times are in agreement with the results published in [30], where τ = 7.63 ps or 5.78 ps. Hence, the estimations carried out in this work support the molecular mechanism suggested for proton moving through successive Zundel cation positions in the confined water of the protonated TPP aggregates in aqueous solution.

Conclusion

The features of the vibrational spectra demonstrate that $H_5O_2^+$ incorporated between two TPP molecules stabilize the complex structure keeping it soluble in solution. The deuterium labeling of the clusters allowed to find the 2993, 3009 cm^{-1} doublet in the region of H—O—D stretching vibrations that shape is identical to the doublet at 982, 1000 cm^{-1} found in a thin film without heavy water, so the latter is identified with proton sharing in the O—H^+···O moiety. Zundel-like ion and unique structure of an aqueous coating around the water–porphyrin dimeric complex are responsible for cooperative motions in the self-organizing processes resulting in highly ordered mono-protonated TPP aggregates. This unique structure of water confined in the aggregates is formed due to proton moving along hydrogen bonds of the tetrahedral network bypassing a water molecule neighboring with a Zundel cation, because alternatively hydrogen bonding is not impossible. This molecular mechanism suggested for proton moving through water is supported by the observation of half of tetrahedral angle "molecular track" observed by SEM and by the proton hopping time estimated. The molecular mechanism implies that protons are extended through water as a wave and are trapped by oxygen atoms through hydrogen bonding as a particle. It should be noted that the purity of water used for the aggregates self-assembling influences on the extent of water–porphyrin matrix self-organization in supramolecular structures.

Acknowledgement

The European Union supported this work under the INTAS programme Grant No. 01-2101.

References

[1] D. Marx, M.E. Tuckerman, J. Hutter, M. Parrinello, Nature 397 (1999) 601–604.
[2] K.R. Asmis, N.L. Pivonka, G. Santambrogio, M. Brümmer, C. Kaposta, D.M. Neumark, L. Wöste, Science 299 (2003) 1375–1377.
[3] J.M. Headrick, E.G. Diken, R.S. Walters, N.I. Hammer, R.A. Christie, J. Cui, E.M. Myshakin, M.A. Duncan, M.A. Johnson, K.D. Jordan, Science 308 (2005) 1765–1769.
[4] W. Kulig, N. Agmon, Nat. Chem. 5 (2013) 29–35.
[5] A.V. Udal'tsov, A.V. Bolshakova, J.G. Vos, J. Mol. Struct. 1065–1066 (2014) 170–178, http://dx.doi.org/10.1016/j.molstruc.2014.02.055.
[6] A.V. Udal'tsov, Biochemistry (Moscow) 62 (1997) 1026–1033.
[7] A.V. Udal'tsov, J. Photochem. Photobiol. B: Biol. 37 (1997) 31–39.
[8] A.V. Udal'tsov, V.S. Pshezhetskii, Khim. Fizika 7 (1988) 1656–1660 (in Russian).
[9] A.V. Udal'tsov, L.A. Kazarin, V.A. Sinani, A.A. Sweshnikov, J. Photochem. Photobiol. A: Chem. 151 (2002) 105–119.
[10] V.S. Pshezhetskii, A.V. Udal'tsov, Vysokomolek. Soedin. A 30 (1988) 1470–1475 (in Russian).
[11] A.V. Udal'tsov, A.A. Churin, Internet Photochem. Photobiol. (1998). <http://www.photobiology.com/IUPAC98/Udaltsov/index.htm>.
[12] A.V. Udal'tsov, L.A. Kazarin, A.A. Sweshnikov, J. Mol. Struct. 562 (2001) 227–239.
[13] M.F. Chaplin, Hydrogen ions: <http://www.lsbu.ac.uk/water/>.
[14] N.B. Librovich, V.P. Sakun, N.D. Sokolov, in: N.D. Sokolov (Ed.), Hydrogen Bond, Nauka, Moscow, 1981, pp. 174–211 (in Russian).
[15] A.V. Udal'tsov, G. Kaupp, A.I. Taskaev, Colloid J. 66 (2004) 489–494.
[16] G. Zundel, Hydration and Intermolecular Interactions, Mir, Moscow, 1972 (in Russian).
[17] K. Nakanishi, Infrared Absorption Spectroscopy, Practical, Holden-Day Inc., Nankodo Company Ltd., San Francisco, Tokyo, 1962 (in Russian).
[18] N.P. Perera, K.R. Fega, C. Lawrence, E.J. Sundstrom, J. Tomlinson-Phillips, Dor Ben-Amotz, Proc. Natl. Acad. Sci. USA 106 (2009) 12230–12234.
[19] Yu.I. Naberukhin, Structural Models of Liquids, NSU Press, Novosibirsk, 1981 (in Russian).
[20] M.F. Chaplin, Grotthuss mechanism: <http://www.lsbu.ac.uk/water/grotthuss.html>.
[21] F.H. Stillinger, Science 209 (1980) 451–457.
[22] D. Marx, ChemPhysChem 7 (2006) 1848–1870.
[23] S. Glasstone, K. Laidler, H. Eyring, Theory of Absolute Rates of Reactions, Inostr. Literature Publ., Moscow, 1948, p. 583 (in Russian).
[24] F.H. Stillinger, in: H. Eyring, D. Henderson (Eds.), Theoretical Chemistry: Advances and Perspectives, Acad. Press, New York, etc., 1978, pp. 178–234.
[25] V.A. Rabinovich, Z.Ya. Khavin, Shortened Chemical Handbook, Khimia, Leningrad, 1977 (in Russian).
[26] E.S. Stoyanov, I.V. Stoyanova, C.A. Reed, J. Am. Chem. Soc. 132 (2010) 1484–1485.
[27] T.D. Fridgen, T.B. McMahon, L. MacAleese, J. Lemaire, P. Maitre, J. Phys. Chem. A 108 (2004) 9008–9010.
[28] N.K. Roberts, H.L. Northey, J. Chem. Soc., Faraday Trans. I (70) (1974) 253–262.
[29] J.H. Simpson, H.Y. Carr, Phys. Rev. 111 (1958) 1201–1202.
[30] P. Choi, N.H. Jalani, R. Datta, J. Electrochem. Soc. 152 (2005) E123–E130.